Organic Electronics 14 (2013) 2925–2931

Contents lists available at ScienceDirect

Organic Electronics

journal homepage: www.elsevier.com/locate/orgel

Charge carrier mobility through vacuum–sublimed glassy films of *s*-triazine- and carbazole-based bipolar hybrid and unipolar compounds

Qiang Wang [a], Jason U. Wallace [b], Thomas Y.-H. Lee [a], Lichang Zeng [a,1], Jane J. Ou [a], Shaw H. Chen [a,c,*]

[a] Department of Chemical Engineering, University of Rochester, Rochester, NY 14627, USA
[b] Department of Mathematics and Natural Sciences, D'Youville College, Buffalo, NY 14201, USA
[c] Laboratory for Laser Energetics, University of Rochester, Rochester, NY 14623, USA

ARTICLE INFO

Article history:
Received 1 July 2013
Received in revised form 16 August 2013
Accepted 18 August 2013
Available online 3 September 2013

Keywords:
Bipolar and unipolar organic compounds
Vacuum–sublimed glassy films
Charge-carrier mobility

ABSTRACT

Instead of physical mixtures as bipolar charge transport media for organic electronics, chemical hybrids comprising non-conjugated spacers are explored to strive for miscibility and morphological stability. Bipolar **TRZ-3Cz(MP)2** and **TRZ-1Cz(MP)2** as well as unipolar **C3-2TRZ(2*t*Bu)**, **C2-2TRZ(2*t*Bu)** and **C3-2Cz(MP)2** were synthesized with propylene or ethylene spacers serving to decouple the Cz(MP)2 and TRZ moieties. Glassy films were prepared by vacuum sublimation for the characterization of transport properties using the photocurrent time-of-flight technique. The results indicate that both the TRZ:Cz(MP)2 ratio and the spacer length enable charge-carrier mobility to be modulated across orders of magnitude. The **C2-2TRZ(2*t*Bu)** film exhibits the highest electron mobility of all the unipolar TRZ-based glassy films reported to date.

1. Introduction

Organic semiconductors have been actively explored for potential applications to full-color displays [1], solid-state lighting [2], and solar cells [3] to take advantage of their lightweight, large-area fabrication, low processing cost, and mechanical flexibility. Charge transport through semiconducting films is one of the critical parameters affecting device performance. Effective charge transport entails hopping from one molecule to another without being trapped or scattered. Charge traps resulting from impurities or defects may act as localized low-energy sites that can immobilize charge carriers, thus depressing mobility [4]. Favorable molecular packing is known to facilitate charge transport through improved overlap of electronic wavefunctions [5]. Single crystalline materials possess superior charge carrier mobility, but their practical application is hampered by inherent difficulty with large-area fabrication [6]. Mobility in polycrystalline materials increases with domain size because of fewer grain boundaries to trap charge carriers [7]. While not as effective charge transport media as crystalline materials, amorphous materials offer isotropic and homogeneous properties without grain boundaries across sizable glassy films. Balanced hole and electron fluxes through the emitting layer in an organic light-emitting diode are known to yield superior device efficiency and lifetime [8]. Charge carrier mobility can be tuned in principle to balance charge fluxes by mixing hole- and electron-transport components (HTMs and ETMs) [9], but potential phase separation with simultaneous crystallization may adversely affect long-term device stability. Charge transport capability could be modulated by coupling HTMs directly with ETMs at the expense of modifying

* Corresponding author at: Department of Chemical Engineering, University of Rochester, Rochester, NY 14627, USA. Tel.: +1 585 275 0909.
E-mail address: shch@LLE.rochester.edu (S.H. Chen).
[1] Current address: Universal Display Corporation, 375 Phillips Boulevard, Ewing, NJ 08618, USA

1566-1199/$ - see front matter © 2013 Elsevier B.V. All rights reserved.
http://dx.doi.org/10.1016/j.orgel.2013.08.017

their HOMO and LUMO levels while depressing triplet energies, E_T[10,11].

As an alternative approach, chemical hybrids comprising HTMs and ETMs linked through a non-conjugated spacer, *viz.* a series of C–C σ-bonds, would retain the HOMO and LUMO levels and the high E_T values inherent to the independent moieties [12]. The insertion of a spacer has been demonstrated to prevent phase separation with enhanced stability of glassy films against undesired crystallization, thereby improving the PhOLED's temporal stability [13], in addition to suppressing charge-transfer complex formation relative to the ***p***- and ***m***-linked hybrids [14] shown to suffer an adverse effect on external quantum efficiency. To illustrate this idea, a series of bipolar hybrid and unipolar compounds comprising carbazole (Cz) and *s*-triazine (TRZ) were synthesized for a systematic investigation of charge transport properties in relation to chemical composition via synthesis and calculation of intermolecular packing behaviors. The present work was further motivated by Cz- and TRZ-derivatives possessing potentially useful hole and electron mobility values from 10^{-7} to 10^{-2} and 10^{-5} to 10^{-3} cm^2/V s, respectively, with HOMO and LUMO levels suitable for charge injection in OLEDs [1,15–17].

2. Experimental section

2.1. Material synthesis and characterization

Synthesis, purification, and analytical data are described in the Supporting Information. ^1H NMR spectra were acquired in $CDCl_3$ with an Avance-400 spectrometer (400 MHz) at 298 K using tetramethylsilane as an internal standard. Elemental analysis was carried out at the Elemental Analysis Facility, University of Rochester. Molecular weights were measured with a MALDI-TOF mass spectrometer (Brüker Autoflex III) with trans-3-indoleacrylic acid (IAA) as the matrix.

2.2. Electrochemical characterization

Cyclic voltammetry, CV, was conducted in an EC-Epsilon potentiostat (Bioanalytical Systems Inc.). A silver/silver chloride (Ag/AgCl) wire, a platinum wire, and a glassy carbon disk with a diameter of 3 mm were used as the reference, counter, and working electrodes, respectively. Samples were dissolved at a concentration of 10^{-3} M in acetonitrile:toluene at 1:1 by volume containing 0.1 M tetraethylammonium tetrafluoroborate as the supporting electrolyte. Acetonitrile and toluene were freshly distilled over calcium hydride and sodium with benzophenone, respectively. The dilute sample solutions exhibit reduction and oxidation scans against the Ag/AgCl reference electrode. The reduction and oxidation potentials were adjusted to ferrocene (Fc) as an internal standard with an oxidation potential of 0.51 ± 0.02 V over Ag/AgCl. The resulting reduction and oxidation potentials, $E_{1/2}$(red) and $E_{1/2}$(oxd), relative to (Fc/Fc^+) were used to calculate the LUMO and HOMO levels in solution and neat film as presented in Table S1.

2.3. Solid morphology and phase transition temperatures

Phase transition temperatures were determined by differential scanning calorimetry (DSC, Perkin–Elmer DSC-7) with a continuous nitrogen purge at 20 ml/min. Samples were preheated to above their melting temperatures and then cooled down to −30 °C at −100 °C/min before the reported second heating and cooling scans were recorded at ±20 °C/min. The nature of the phase transitions was characterized by hot-stage polarizing optical microscopy (POM, DMLM, Leica, FP90 central processor and FP82 hot stage, Mettler Toledo).

2.4. Thin film preparation and characterization

Thin films for the characterization of absorption and morphology were prepared by vacuum sublimation on fused silica substrates (International Crystal Laboratories) at 1 nm/s under 5×10^{-6} torr. Film thicknesses were determined by a stylus-type profilometer (XP-200, Ambios technology). Absorption spectra of films were acquired with a UV–Vis–NIR spectrophotometer (Lambda 900, Perkin–Elmer). The optical micrographs of organic films were produced with a digital camera (MicroPix C-1024) mounted on a polarizing optical microscope (Leitz Orthoplan-Pol). The **C2-2TRZ(2*t*Bu)** films for electron diffraction were prepared by vacuum sublimation under the afore-mentioned condition on a NaCl substrate (International Crystal Laboratories), and then was covered with an amorphous PVP film spin-cast from a 0.5 wt% methanol solution at 4000 rpm. An absorbance of 0.005 optical density unit, equivalent to 99% transmittance, was found independently for the 40-nm-thick PVP film at 266 nm. The resulting PVP/**C2-2TRZ(2*t*Bu)**/NaCl stack was subjected to 266 nm laser pulses after passing through a fused silica substrate coated with a Ag layer to simulate the condition of a TOF measurement. The film was finally floated off in deionized water, caught with copper grids, and characterized with a transmission electron microscope (FEI Tecnai F20).

2.5. TOF device fabrication and characterization

The absorption spectra of neat solid films of **C3-2Cz(MP)2**, **C2-2TRZ(2*t*Bu)**, **C3-2TRZ(2*t*Bu)**, **TRZ-1Cz(MP)2**, and **TRZ-3Cz(MP)2** films are shown in Fig. S1a. Glass substrates coated with patterned ITO were thoroughly cleaned and treated with oxygen plasma prior to use. Two device structures were employed: Al/organic layer/ITO for **C3-2Cz(MP)2**, **TRZ-1Cz(MP)2** and **TRZ-3Cz(MP)2**, and Ag/organic layer/ITO for **C2-2TRZ(2*t*Bu)** and **C3-2TRZ(2*t*Bu)** for characterization by the photocurrent TOF system described in Fig. S1b[18]. The organic layers were prepared by thermal vacuum deposition onto ITO-coated substrates at 1 nm/s to yield a film thickness of 6–12 μm as determined by a stylus-type profilometer (XP-200, Ambios technology), preferably greater than the penetration depth by more than one order of magnitude as commonly practiced [19]. The devices were completed by thermal vacuum deposition of 30-nm-thick silver for **C2-2TRZ(2*t*Bu)** and **C3-2TRZ(2*t*Bu)** or 100-nm-thick aluminum for **C3-2Cz(MP)2**, **TRZ-1Cz(MP)2** and **TRZ-3Cz(MP)2** at 1 nm/s

through a shadow mask to define an active area of 0.1 cm^2. All vacuum deposition processes were carried out at a base pressure less than 5×10^{-6} torr. A power supply (Hewlett Packard 6110A, DC) was connected to the device's semi-transparent electrode, through which a nitrogen laser (Photochemical Research Associates, $\lambda = 337$ nm, pulse duration = 800 ps FWHM) for **C3-2Cz(MP)2**, **TRZ-1Cz(MP)2** and **TRZ-3Cz(MP)2**, or the fourth harmonic generation of a Nd:YAG laser (GCR-100, Quanta-Ray Spectra-Physics, $\lambda = 266$ nm, pulse duration = 4–5 ns FWHM) for **C2-2TRZ(2*t*Bu)** and **C3-2TRZ(2*t*Bu)** was used as photoexcitation. A load resistor was connected to the other electrode and an oscilloscope (Tektronix TDS 2024B, 200 MHz) measured the voltage drop, yielding the photocurrent transient. Measurements were carried out in a vacuum chamber furnished with an appropriate window (LTS-22-1CH). The TOF measurement of mobility in organic semiconductors was reported to carry a typical error of 20% [20].

3. Results and discussion

Carbazole and *s*-triazine were employed as building blocks for the construction of bipolar hybrid and unipolar compounds to elucidate the effect of molecular structure on charge carrier mobility. The ethylene and propylene spacers were inserted to ensure material processing into morphologically stable glassy films and to decouple the two π-systems to retain their independent HOMO and LUMO levels. Depicted in Chart 1 are the molecular structures of model compounds synthesized following the reaction scheme and purification procedures with analytical data, all presented in the Supporting Information. The compounds with propylene spacers were synthesized by treating Cz(MP)2 or TRZ carrying an allyl group with 9-BBN for the subsequent Suzuki coupling reaction. The compound with an ethylene spacer, *i.e.***C2-2TRZ(2*t*Bu)**, was synthesized following a divergent route starting with 1,2-bis(4-bromo-phenyl)ethane. As shown in Fig. S2, all the compounds exhibit single steps characteristic of glass transition except **C2-2TRZ(2*t*Bu),** which on heating undergoes two-stage crystallization at 185 and 361 °C above its glass transition temperature (T_g) at 148 °C.

Vacuum–sublimed thin film morphologies of all the compounds in TOF devices were verified as amorphous under POM before and after mobility measurements (Fig. S3a). All these organic films in the TOF device remained amorphous when left at room temperature for two months, a manifestation of morphological stability. Seemingly inclined to crystallization based on DSC scans, **C2-2TRZ(2*t*Bu)** was further investigated with transmission electron microscopy. A freshly prepared stack of PVP/**C2-2TRZ(2*t*Bu)**/NaCl was subjected to incident 266 nm laser pulses as conducted in a TOF measurement. Upon dissolving the PVP layer and NaCl in deionized water, the isolated **C2-2TRZ(2*t*Bu)** film was characterized by electron diffraction, showing a typical amorphous halo (Fig. S3b). The TOF transients are illustrated for **TRZ-3Cz(MP)2** in Fig. S4, where the transit time can be determined by the point at which the photocurrent starts to drop from a plateau on a linear plot with time. It is difficult, however, to extract transit time from dispersive hole and electron photocurrents in the linear plot; the rest of compounds exhibit a similar behavior. In practice, a log–log plot of photocurrent with time enables the transit time to be readily determined by the two intersecting dashed straight lines (insets in Fig. S4) to obtain unambiguous data in all cases. The accessible range of electric field is limited by electric ringing,

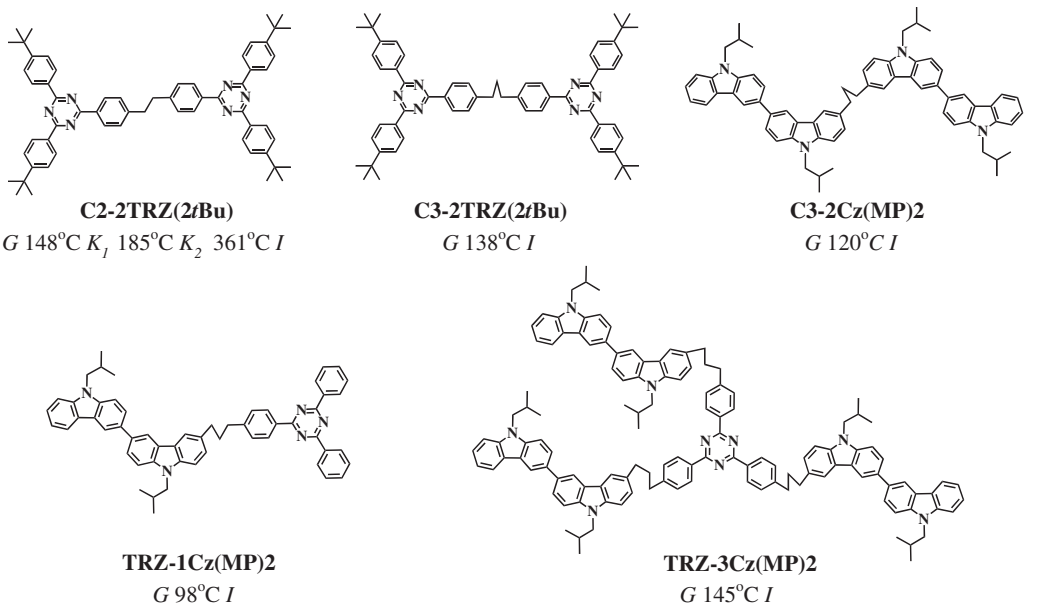

Chart 1. Molecular structures with their thermal transition temperatures determined by DSC second heating scans of samples preheated to beyond their crystalline melting points. Symbols: *G*, glassy; *K*, crystalline and *I*, isotropic.

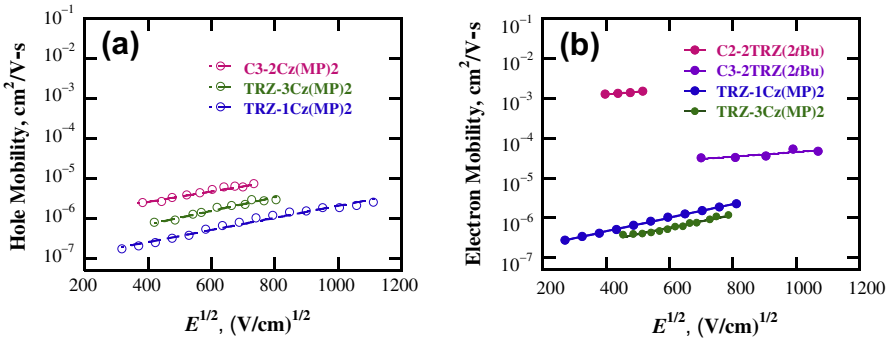

Fig. 1. (a) Hole and (b) electron mobilities as functions of electric field ($E^{1/2}$) for **TRZ-1Cz(MP)2**, **TRZ-3Cz(MP)2**, **C3-2Cz(MP)2**, **C2-2TRZ(2*t*Bu)**, and **C3-2TRZ(2*t*Bu)** in ITO/organic layer/Al or ITO/organic layer/Ag devices. Vanishing values of hole and electron mobility are not shown in (a) and (b) for **C2-2TRZ(2*t*Bu)**, **C3-2TRZ(2*t*Bu)**, and **C3-2Cz(MP)2**. The data points are accompanied by an average error of ±8%.

thus preventing measurements on time scales shorter than 100 ns. In addition, a high applied voltage may cause shorting in TOF devices.

As shown in Fig. 1, the Poole–Frenkel relationship [21] is obeyed by **TRZ-1Cz(MP)2**, **TRZ-3Cz(MP)2**, **C3-2Cz(MP)2**, **C3-2TRZ(2*t*Bu)**, and **C2-2TRZ(2*t*Bu)**. The hole mobility values of **C3-2Cz(MP)2**, **TRZ-3Cz(MP)2**, and **TRZ-1Cz(MP)2** decrease with a decreasing Cz content, and so do the electron mobility values of **C3-2TRZ(2*t*Bu)**, **TRZ-1Cz(MP)2**, and **TRZ-3Cz(MP)2** with a decreasing TRZ content. Because of the weaker current signal caused in part by the less efficient charge generation, higher fields were needed for the measurement of mobility through the **C3-2TRZ(2*t*Bu)** films compared to the rest of the compounds. No hole currents were detectable for **C3-2TRZ(2*t*Bu)** and no electron currents were detectable for **C3-2Cz(MP)2** across the same range of applied field. The characterization of HOMO and LUMO levels of the bipolar and unipolar compounds as follows is intended to demonstrate the modulation of charge-carrier mobility by varying the TRZ:Cz(MP)2 ratio without altering their HOMO and LUMO levels. The oxidation and reduction potentials were characterized by CV, as displayed in Fig. S5, with the results presented in Table S1 for energy levels in both solution and neat solid film using equations based on various solvents including dichloromethane, acetonitrile, and DMF [22,23]. Protected or not at the 3-, 6-, and/or 9- (*i.e. N*-) positions, carbazole has been reported to suffer oxidative instability [24,25]. This problem, however, appears to be absent up to the second oxidation and reduction scans in support of experimental reproducibility of the reported energy levels for Cz(MP)2, **C3-2Cz(MP)2**, **TRZ-1Cz(MP)2**, and **TRZ-3Cz(MP)2**. Because of the absence of π-conjugation between the two moieties across the propylene spacer, the HOMO and LUMO levels of **TRZ-1Cz(MP)2** and **TRZ-3Cz(MP)2** are essentially imported from those of Cz(MP)2 and TRZ, respectively. It is worth noting that HOMO and LUMO levels are relatively close to those of commonly used hole- and electron-transport materials in OLEDs, such as NPB at −5.4 eV [26] and Alq3 at −2.3 eV [23], respectively.

It is also noted that unipolar **C3-2Cz(MP)2** possesses a hole mobility about an order of magnitude higher than the two bipolar hybrids, all with propylene spacers. Similarly, unipolar **C3-2TRZ(2*t*Bu)** exhibits an electron mobility about an order of magnitude higher than the two bipolar hybrids. These observations are a manifestation of concentration effect in transition from bipolar hybrids to unipolar compounds with the same spacer length. Shortening the spacer from propylene to ethylene enhances the electron mobility of **C2-2TRZ(2*t*Bu)** over that of **C3-2TRZ(2*t*Bu)** by about two orders of magnitude, likely contributed by better molecular packing involving the former that cannot be readily characterized as experimental validation. For the visualization of molecular packing including π-stacking, dynamic simulations of multi-molecular systems were attempted as an alternative approach, as reported previously for chiral assemblies of oligofluorenes with enantiomeric pendants [27], but failed to converge presumably because of the insufficient system size and simulation time. Instead, the Gaussian 09 software package was used to calculate optimized single molecular structures. The results displayed in Fig. 2 suggest that the energetically favored linear *anti*-conformation across the ethylene spacer and the co-planarity of the two TRZ groups in **C2-2TRZ(2*t*Bu)** are responsible for effective molecular packing in favor of charge transport. In contrast, the angular conformation of **C3-2TRZ(2*t*Bu)** does not allow molecular packing as effective as **C2-2TRZ(2*t*Bu)**. Inadequate as it is for the description of a real chemical system in solid state, single molecular calculation is shown to be capable of acquiring optimized conformations as a qualitative assessment of relative charge transport properties.

To evaluate **C2-2TRZ(2*t*Bu)** against existing TRZ-derivatives in terms of electron mobility, previously reported compounds capable of vacuum sublimation into glassy films were identified in Table 1 and Fig. 3a along with their T_g values [17,28]. As a benchmark of electron mobility, the most frequently used Alq3 [28] with a T_g at 177 °C [29] is included for a comparison in Fig. 3b. It is quite encouraging that **C2-2TRZ(2*t*Bu)** exhibits the highest electron mobility of all, including those that are not accommodated in Fig. 3b for the sake of clarity in comparing data from additional sources [16,30,31]. The difference in film thickness is deemed inconsequential in view of the established film thickness independence up to 10 μm [32–36].

Phosphorescent OLEDs, ITO/MoO_3(10 nm)/emitting layer(40–50 nm)/1,3,5-tris(N-phenylbenz-imidazol-2-yl)-benzene (30 nm)/CsF(1 nm)/Al(100 nm) with an emitting

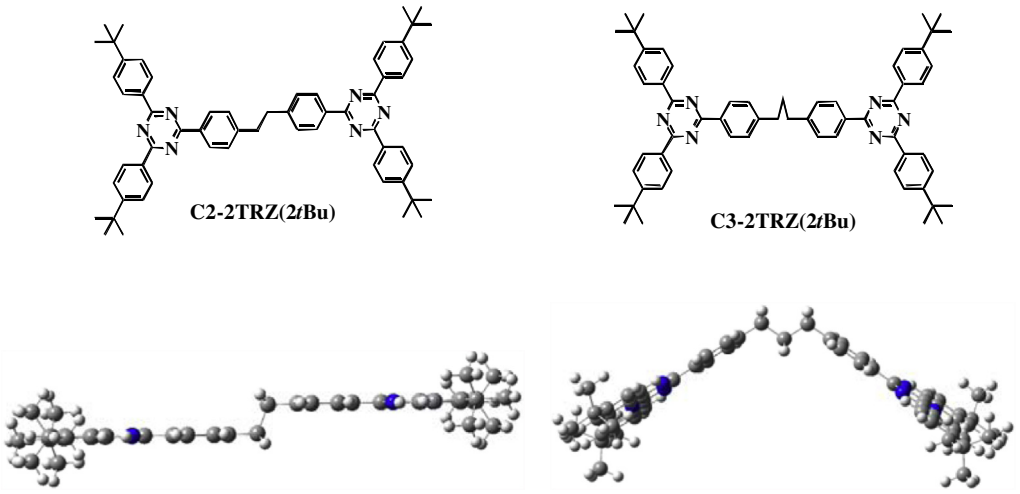

Fig. 2. Single molecular structures of **C2-2TRZ(2*t*Bu)** and **C3-2TRZ(2*t*Bu)** optimized with Gaussian 09 using B3LYP functional with the 6-31G(d) basis set.

Table 1
Film thicknesses, electron and hole mobility data compiled in Fig. 3 with vacuum–sublimed films of compounds **A** through **C**, **Alq3**, and **C2-2TRZ(2*t*Bu)**.

Compound	Film thickness (μm)	Device structure	Data source
A	2–3	Ag (30 nm)/**A**/Al (150 nm)	Ref. [17]
B	2–3	Ag (30 nm)/**B**/Al (150 nm)	*Ibidem*
C	0.2	ITO/NPB/Alq3:C545T/**C**/CuPc/NPB/Alq3/Ag	Ref. [28]
Alq3	0.2	ITO/NPB/Alq3:C545T/**Alq3**/CuPc/NPB/Alq3/Ag	*Ibidem*
C2-2TRZ(2*t*Bu)	12	Ag (30 nm)/**C2–2TRZ(2*t*Bu)**/Al (100 nm)	Present work

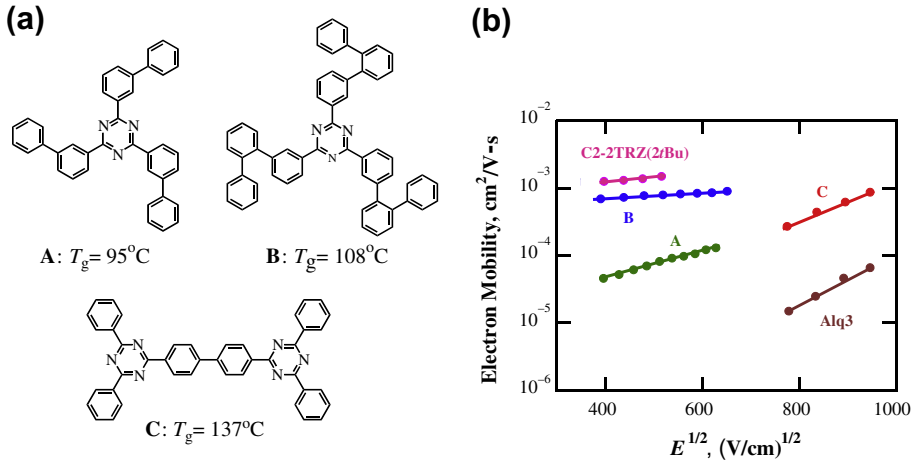

Fig. 3. (a) Molecular structures of unipolar TRZ-based compounds for which electron mobility values have been reported for vacuum–sublimed glassy films, and (b) comparison of their electron mobility values with that of **Alq3** and **C2-2TRZ(2*t*Bu)**.

layer consisting of **TRZ-1Cz(MP)2** and **TRZ-3Cz(MP)2** doped with 10 wt% $Ir(mppy)_3$, were reported in our previous study [12]. The relatively low current efficiency of 18 cd/A at 10 mA/cm^2 with **TRZ-1Cz(MP)2** was attributed to the recombination zone being close to the anode as a result of the slightly greater electron mobility than hole and the electron-transport capability of $Ir(mppy)_3$ as the dopant. At the same doping level and the same charge injection barriers into the emitting layers comprising the two distinct hybrids (Table S1), the higher hole mobility and the lower electron mobility of **TRZ-3Cz(MP)2** than those of **TRZ-1Cz(MP)2** as observed here must have shifted the recombination zone away from the anode, thereby improving the current efficiency to 28 cd/A at 10 mA/cm^2. The satisfactory interpretation of relative current efficiency values

is an illustration of the relevance of the observed mobility data to PhOLED devices.

4. Conclusions

Non-conjugated bipolar hybrid compounds, **TRZ-1Cz(MP)2** and **TRZ-3Cz(MP)2**, with variable TRZ:Cz(MP)2 ratios and unipolar compounds, **C3-2Cz(MP)2**, **C3-2TRZ(2*t*Bu)**, and **C2-2TRZ(2*t*Bu)**, were characterized by the photocurrent TOF technique. Alkylene spacers were incorporated in these compounds to improve morphological stability against crystallization and to electronically decouple the two π-systems with an aim of retaining independent energy levels. The vacuum–sublimed films of these compounds in TOF devices were characterized as amorphous by polarizing optical microscopy and transmission electron microscopy as needed. Hole mobility increases from **TRZ-1Cz(MP)2**, **TRZ-3Cz(MP)2** to **C3-2Cz(MP)2** over a factor of about 10, while electron mobility increases from **TRZ-3Cz(MP)2**, **TRZ-1Cz(MP)2** to **C2-2TRZ(2*t*Bu)** over a factor of more than 10^3. The broad ranges of mobility are likely caused by the difference in molecular packing beyond the TRZ:Cz(MP)2 ratio that defy experimental verification in glassy films at present. Based on the optimized single molecular structures acquired by Gaussian 09, the linear *anti*-conformation across the ethylene spacer and the co-planarity between the two TRZ groups result in effective molecular packing in **C2-2TRZ(2*t*Bu)**, while the angular conformation of **C3-2TRZ(2*t*Bu)** prevents as effective molecular packing. In a nutshell, the concept of non-conjugated spacer has proven to be a powerful tool for designing potentially useful charge transport media with predictable morphological, molecular orbital energy levels, and tunable charge transport capability by varying chemical composition and molecular conformation.

Acknowledgments

The authors are grateful to Professors Ching W. Tang and Lewis J. Rothberg and Mr. Millard Wyman for technical advice as well as access to photocurrent TOF device fabrication and characterization facilities. They acknowledge the financial support by the Department of Energy under Grant No. DE-EE0003296 for a solid-state lighting team project. Additional funding was provided by the Department of Energy Office of Inertial Confinement Fusion under Co-operative Agreement No. DE-FC52-08NA28302 with Laboratory for Laser Energetics at the University of Rochester. The support of DOE does not constitute an endorsement by DOE of the views expressed in this article.

Appendix A. Supplementary material

Reaction scheme for synthesis, purification procedures, and analytical data to validate molecular structures of **C3-2Cz(MP)2**, **C2-2TRZ(2*t*Bu)**, and **C3-2TRZ(2*t*Bu)**. Absorption spectra of **C3-2Cz(MP)2**, **C2-2TRZ(2*t*Bu)**, **C3-2TRZ(2*t*Bu)**, **TRZ-1Cz(MP)2**, and **TRZ-3Cz(MP)2** films; the schematic diagram of the TOF apparatus; DSC heating and cooling scans of **C3-2Cz(MP)2**, **C2-2TRZ(2*t*Bu)**, **C3-2TRZ(2*t*Bu)**, **TRZ-1Cz(MP)2**, and **TRZ-3Cz(MP)2**, all pretreated to eliminate thermal history; polarizing optical micrographs of **C2-2TRZ(2*t*Bu)**, **C3-2TRZ(2*t*Bu)**, **C3-2Cz(MP)2**, **TRZ-1Cz(MP)2**, and **TRZ-3Cz(MP)2** films in TOF devices before and after mobility measurements; electron diffraction pattern of a vacuum–sublimed **C2-2TRZ(2*t*Bu)** film after eight 266 nm laser exposures, the same treatments as through TOF measurement; representative TOF transients of **TRZ-3Cz(MP)2**; cyclic voltammograms of Cz(MP)2, TRZ, **C3-2Cz(MP)2**, **TRZ-1Cz(MP)2**, **TRZ-3Cz(MP)2**, **C2-2TRZ(2*t*Bu)**, and **C3-2TRZ(2*t*Bu)** in acetonitrile:toluene at 1:1 by volume; and HOMO and LUMO levels for TRZ, Cz(MP)2, bipolar hybrid and unipolar compounds. Supplementary data associated with this article can be found, in the online version, at http://dx.doi.org/10.1016/j.orgel.2013.08.017.

References

[1] L. Xiao, Z. Chen, B. Qu, J. Luo, S. Kong, Q. Gong, J. Kido, Adv. Mater. 23 (2011) 926.
[2] M.C. Gather, A. Köhnen, K. Meerholz, Adv. Mater. 23 (2011) 233.
[3] A.W. Hains, Z. Liang, M.A. Woodhouse, B.A. Gregg, Chem. Rev. 110 (2010) 6689.
[4] D. Poplavskyy, W. Su, F. So, J. Appl. Phys. 98 (2005) 014504.
[5] V. Coropceanu, J. Cornil, D.A. da Silva Filho, Y. Olivier, R. Silbey, J.-L. Brédas, Chem. Rev. 107 (2007) 926.
[6] Y. Shirota, H. Kageyama, Chem. Rev. 107 (2007) 953.
[7] G. Horowitz, M.E. Hajlaoui, Adv. Mater. 12 (2000) 1046.
[8] R. Meerheim, S. Scholz, S. Olthof, G. Schwartz, S. Reineke, K. Walzer, K. Leo, J. Appl. Phys. 104 (2008) 014510.
[9] G. Schwartz, T.-H. Ke, C.-C. Wu, K. Walzer, K. Leo, Appl. Phys. Lett. 93 (2008) 073304.
[10] (a) C.-H. Chen, W.-S. Huang, M.-Y. Lai, W.-C. Tsao, J.T. Lin, Y.-H. Wu, T.-H. Ke, L.-Y. Chen, C.-C. Wu, Adv. Funct. Mater. 19 (2009) 2661; (b) S.-J. Su, C. Cai, J. Kido, Chem. Mater. 23 (2011) 274.
[11] (a) W. Jiang, L. Duan, J. Qiao, A. Wang, Y. Qiu, Org. Lett. 13 (2011) 3146; (b) S.-H. Cheng, S.-H. Chou, W.-Y. Hung, H.-W. You, Y.-M. Chen, A. Cheskar, Y.-H. Liu, K.-T. Wong, Org. Electron. 14 (2013) 1086.
[12] L. Zeng, T.Y.-H. Lee, P.B. Merkel, S.H. Chen, J. Mater. Chem. 19 (2009) 8772.
[13] T.Y.-H. Lee, Q. Wang, J.U. Wallace, S.H. Chen, J. Mater. Chem. 22 (2012) 23175.
[14] Q. Wang, J.U. Wallace, T.Y-H. Lee, J.J. Ou, Y.-T. Tsai, Y.-H. Huang, C.-C. Wu, L.J. Rothberg, S.H. Chen, J. Mater. Chem. C 1 (2013) 2224.
[15] K. Brunner, A. van Dijken, H. Börner, J.J.A.M. Bastiaansen, N.M.M. Kiggen, B.M.W. Langeveld, J. Am. Chem. Soc. 126 (2004) 6035.
[16] T. Matsushima, M. Takamori, Y. Miyashita, Y. Honma, T. Tanaka, H. Aihara, H. Murata, Org. Electron. 11 (2010) 16.
[17] H.-F. Chen, S.-J. Yang, Z.-H. Tsai, W.-Y. Hung, T.-C. Wang, K.-T. Wong, J. Mater. Chem. 19 (2009) 8112.
[18] S. Tiwari, N.C. Greenham, Opt. Quant. Electron. 41 (2009) 69.
[19] W.-Y. Hung, T.-H. Ke, Y.-T. Lin, C.-C. Wu, T.-H. Hung, T.-C. Chao, K.-T. Wong, C.-I. Wu, Appl. Phys. Lett. 88 (2006) 064102.
[20] T. Kreouzis, D. Poplavskyy, S.M. Tuladhar, M. Quiles-Campoy, J. Nelson, A.J. Campell, D.D.C. Bradley, Phys. Rev. B 73 (2006) 235201.
[21] W.D. Gill, J. Appl. Phys. 43 (1972) 5033.
[22] B.W. D'Andrade, S. Datta, S.R. Forrest, P. Djurovich, E. Polikarpov, M.E. Thompson, Org. Electron. 6 (2005) 11.
[23] P.I. Djurovich, E.I. Mayo, S.R. Forrest, M.E. Thompson, Org. Electron. 10 (2009) 515.
[24] J.F. Ambrose, R.F. Nelson, J. Electrochem. Soc. 115 (1968) 1159.
[25] J.F. Ambrose, L.L. Carpenter, R.F. Nelson, J. Electrochem. Soc. 122 (1975) 876.
[26] M.E. Kondakova, T.D. Pawlik, R.H. Young, D.J. Giesen, D.Y. Kondakov, C.T. Brown, J.C. Deaton, J.R. Lenhard, K.P. Klubek, J. Appl. Phys. 104 (2008) 094501.
[27] Y. Geng, A. Trajkovska, D. Katsis, J.J. Ou, S.W. Culligan, S.H. Chen, J. Am. Chem. Soc. 124 (2002) 8337.
[28] R.A. Klenkler, H. Aziz, A. Tran, Z.D. Popovic, G. Xu, Org. Electron. 9 (2008) 285.

[29] L.S. Sapochak, A. Padmaperuma, N. Washton, F. Endrino, G.T. Schmett, J. Marshall, D. Fogarty, P.E. Burrows, S.R. Forrest, J. Am. Chem. Soc. 123 (2001) 6300.
[30] T. Ishi-i, K. Yaguma, T. Thiemann, M. Yashima, K. Ueno, S. Mataka, Chem. Lett. 33 (2004) 1244.
[31] H. Aihara, N. Yanai, T. Yamakawa, T. Tanaka, M. Sato, Trans. Mater. Res. Soc. Jpn. 32 (2007) 333.
[32] S.C. Tse, H.H. Fong, S.K. So, J. Appl. Phys. 94 (2003) 2033.
[33] H.H. Fong, A. Papadimitratos, G.G. Malliaras, Appl. Phys. Lett. 89 (2006) 172116.
[34] S. Gambino, A.K. Bansal, I.D.W. Samuel, Org. Electron. 11 (2010) 467.
[35] S.V. Novikov, A.P. Tyutnev, L.B. Schein, Chem. Phys. 403 (2012) 68.
[36] O.J. Weiβ, R.K. Krause, A. Hunze, J. Appl. Phys. 103 (2008) 043709.